CT Radiomics and Clinical Feature Model to Predict Lymph Node Metastases in Early-Stage Testicular Cancer

Catharina Silvia Lisson *, Sabitha Manoj, Daniel Wolf, Jasper Schrader, Stefan Andreas Schmidt, Meinrad Beer, Michael Goetz, Friedemann Zengerling, Christoph Gehard Lisson

Posted Date: 2 February 2023

doi: 10.20944/preprints202302.0025.v1

Keywords: radiomics signature; prediction; machine learning; testicular cancer; personalised oncology; precision imaging

Article

CT Radiomics and Clinical Feature Model to Predict Lymph Node Metastases in Early-Stage Testicular Cancer

Catharina Silvia Lisson [1,2,3,*], Sabitha Manoj [1,3,4], Daniel Wolf [1,3,4], Jasper Schrader [5], Stefan Andreas Schmidt [1,2,3], Meinrad Beer [1,2,3,6,7], Michael Goetz [1,3,8], Friedemann Zengerling [5,†] and Christoph Gerhard Lisson [1,†]

1 Department of Diagnostic and Interventional Radiology, University Hospital of Ulm, Albert-Einstein-Allee 23, 89081 Ulm, Germany; sabitha.manoji@uni-ulm.de (S.M.); daniel.wolf@uni-ulm.de (D.W.); jasper.schrader@uni-ulm.de (J.S.); stefan.schmidt@uniklinik-ulm.de (S.A.S.); meinrad.beer@uniklinik-ulm.de (M.B.); michael.goetz@uni-ulm.de (M.G.); christoph.lisson@uniklinik-ulm.de

2 ZPM – Center for Personalized Medicine, University Hospital of Ulm, Albert-Einstein-Allee 23, 89081 Ulm, Germany

3 XAIRAD – Artificial Intelligence in Experimental Radiology, University Hospital of Ulm, Albert-Einstein-Allee 23, 89081 Ulm, Germany

4 Visual Computing Group, Institute of Media Informatics, Ulm University, James-Franck-Ring, 89081 Ulm, Germany

5 Department of Urology, University Hospital of Ulm, Albert-Einstein-Allee 23, 89081 Ulm, Germany; Friedemann.zengerling@uniklinik-ulm.de (F.Z.)

6 MoMan – Center for Translational Imaging, Department of Internal Medicine II, University Hospital of Ulm, Albert-Einstein-Allee 23, 89081 Ulm, Germany

7 i2SouI – Innovative Imaging in Surgical Oncology Ulm, University Hospital of Ulm, Albert-Einstein-Allee 23, 89081 Ulm, Germany

8 DKFZ – German Cancer Research Center, Division Medical Image Computing, 69120 Heidelberg, Germany

* Correspondence: catharina.lisson@uniklinik-ulm.de; Tel.: +49-731-50061171 OR Michael Goetz

† These authors contributed equally to this work.

Simple Summary: Testicular germ cell tumour (TGCT) is the most common solid cancer in men below 40. The majority present with disease confined to the testis (stage 1), with its primary treatment being radical orchiectomy. Despite the multiple options for managing stage 1 tumours, optimal management is controversial, with further treatment options including active surveillance, chemotherapy and retroperitoneal lymph node dissection. In this study, the authors incorporated quantitative imaging features and clinical risk factors to stratify patients according to lymph node metastases, thus promoting precision imaging in clinical oncology.

Abstract: Accurate retroperitoneal lymph node metastasis (LNM) prediction in early-stage testicular germ cell tumours (TGCT) harbours the potential to significantly reduce over- or undertreatment and treatment-related morbidity in this group of young patients as an important survivorship imperative. We investigated the role of computed tomography (CT) radiomics models integrating clinical predictors for the individualized prediction of LNM in early-stage TGCT. Ninety-one patients with surgically proven testicular germ cell tumours and contrast-enhanced CT were included in this retrospective study. Dedicated radiomics software was used to segment 273 retroperitoneal lymph nodes and extract features. After feature selection, radiomics-based machine learning models were developed to predict LN metastasis. The robustness of the procedure was controlled by 10-fold cross-validation. Using multivariable logistic regression modelling, we developed three prediction models: A radiomics-only model, a clinical-only model and a combined radiomics-clinical model. The models' performance was evaluated using the area under the receiver operating characteristic curve (AUC). Finally, decision curve analysis was performed to estimate the clinical usefulness of the predictive model. The radiomics-only model for predicting lymph node

 doi:10.20944/preprints202302.0025.v1

metastasis reached a greater discrimination power than the clinical-only model, with an AUC of 0.84 (± 0.17; 95% CI) vs 0.60 (± 0.22; 95% CI) in our study cohort. The combined model integrating clinical risk factors and selected radiomics features outperformed the clinical-only and the radiomics-only prediction models and showed good discrimination with an area under the curve of 0.94 (± 0.10; 95% CI). The decision curve analysis demonstrated the clinical usefulness of our proposed combined model. The presented combined CT-based radiomics-clinical model represents an exciting non-invasive prediction tool for individualized prediction of LN metastasis in testicular germ cell tumours. Multi-centre validation is required to generate high quality evidence for its clinical application.

Keywords: radiomics signature; prediction; machine learning; testicular cancer; personalised oncology; precision imaging

1. Introduction

Testicular germ cell tumours (TGCTs) are the most common malignancy among men aged 15–40 (1,2). Its characteristic patient population and high cure rate make this disease unique, constituting one of the few success stories in cancer care (3,4). Besides cure, reducing the amount of therapy-related acute and long-term toxicity is the goal of care due to the young age of the TGCT patients and the long-life expectancy following curative therapy (5–10). The main risk factors for TGCTs include cryptorchidism, family or personal history of TGCT and contact with organochlorine compounds (11,12). TGCTs are classified histologically into seminoma and non-seminoma, including pure non-seminoma and mixed germ cell tumours, with seminoma accounting for approximately 55% of all cases with an average age at diagnosis in the fourth decade of life, about eight years later than non-seminoma (12). TGCT are diagnosed by physical examination, testicular ultrasound and specific tumour markers such as alpha-fetoprotein (AFP), beta-hCG (β-hCG) and lactate dehydrogenase (LDH)(13,14).

Retroperitoneal lymph node dissection (RPLND) is the only treatment modality to correctly stage the nodal status of early testicular cancer. However, due to the short- and long-term complications, such as retrograde ejaculation, the implementation of adjuvant chemotherapy regimens and the excellent prognosis with surveillance approaches in stage I disease, RPLND plays a negligible role as the primary treatment of early-stage TGCTs (15).

As there exist no sensitive and specific biomarkers for relapse (16,17), these patients are usually managed with active surveillance (18). Kollmannsberger et al. reported the excellent outcome of active surveillance for clinical stage I NSGCT with an overall relapse rate of 19% at a median follow-up of 62 months and a 5-year disease-specific survival of 99% (4).

TGCT demonstrate a predictable pattern of metastases, with the ipsilateral retroperitoneal lymph nodes being the first site of the metastatic spread in about 95% of the cases.

Thanks to its excellent spatial resolution, the CT is considered suitable for detecting pathologically enlarged lymph nodes; however, it is formally unable to differentiate benign from infiltrated lymph nodes, especially for smaller ones (19). Due to the absence of a validated consensus, the short axis diameter recommended considering a lymph node malignant is usually 7-8 mm, resulting in the most significant AUC with a sensitivity and specificity approaching 70% (20). Conversely, in 30% of the cases, micrometastatic lymph nodes are already present.

The blood-based tumour AFP, β-HCG, and LDH are the most frequently used tumour markers for the management of TGCT (14). However, these markers are not very specific and are only detected in approximately 60% of men with testicular cancer (14,21). And worse, in pure seminoma patients, β-HCG is only useful in less than 20% of patients (22). Furthermore, there exist (non-TGCT related) conditions related to false positive tumour marker elevation, such as liver disease or genetic conditions leading to an increase of AFP or false positive high levels of B-HCG due to heterophile

 doi:10.20944/preprints202302.0025.v1

antibodies (26). In addition, the sensitivity of these markers is limited, and the levels of these markers are usually "normal" in about 40% of men with disease recurrence (23).

Neither imaging nor serum tumour markers nor clinical nomograms have been proven to be adequate predictors for the presence of lymph node metastases (24,25). Nevertheless, suboptimal therapeutical management jeopardises the excellent outcomes of TGCT patients, with either over- or undertreatment being equally harmful.

Advanced medical imaging integrating high-resolution image acquisition, powerful computational technologies and artificial intelligence (AI)—based image analysis enabled researchers to develop the field of radiomics (26,27). This way, data characterisation algorithms detect specific diagnostic image patterns and convert them into quantitative mineable "big data" (28,29).

Amid the requirements of precision medicine, (AI)—based image analysis addresses the challenges of biopsy being non-invasive, repeatable and applicable for difficult-to-reach lesions within the body by generating texture features extracted from a region of interest (ROI), potentially reflecting tumour physiology and radiographic phenotype (30,31).

Many studies have evaluated the diagnostic potential of radiomics for classifying lymph nodes in different cancer types, including gastric, rectal and bladder cancer, with promising results (32–35). Thus, AI-based advanced imaging might deliver novel imaging biomarkers or radiomic signatures to tackle the urgent problem of under- or overtreatment in TGCT patients.

AI-based advanced imaging could provide new imaging biomarkers or radiomic signatures to combat the urgent problem of under- or over-treatment of TGCT patients.

Our study is the first to investigate computed tomography (CT) radiomics models integrating clinical risk factors for the individualized prediction of lymph node metastasis in patients with early-stage TGCT, thus promoting precision imaging in clinical oncology.

Based on these findings above, we hypothesized that:

1) The radiomics features extracted from retroperitoneal lymph nodes might potentially predict TGCT recurrence.

2) Integrating important clinical factors, including age, histotype, AFP, ß-HCG and BMI, into a combined radiomics-clinical model might add an incremental value to predict TGCT recurrence.

2. Materials and Methods

2.1. Patients and Imaging Protocol

In this retrospective study, 91 treatment-naive patients with surgically proven stage I TGCT who underwent contrast-enhanced CT scans at our institution between January 2006 and December 2016 were included. Demographic patient data, laboratory and clinical data, such as tumour markers, disease stage, and clinical outcome data, were recorded by thoroughly reviewing electronic charts and the radiology information system. Exclusion criteria were incomplete clinical and imaging data records and missing histological confirmation.

The primary endpoint was retroperitoneal LN metastases of TGCT based on subsequent clinical assessments and imaging studies. Follow-up recordings in the electronic charts determined each patient's status.

All enrolled TGCT subjects were followed up for at least six years after orchiectomy. Of 167 screened patients, 91 were included in the final study cohort after excluding 76 patients due according to the exclusion criteria. A flow diagram of the cohort selection is presented in Figure 1.

Preprints (www.preprints.org) | NOT PEER-REVIEWED | Posted: 2 February 2023 doi:10.20944/preprints202302.0025.v1

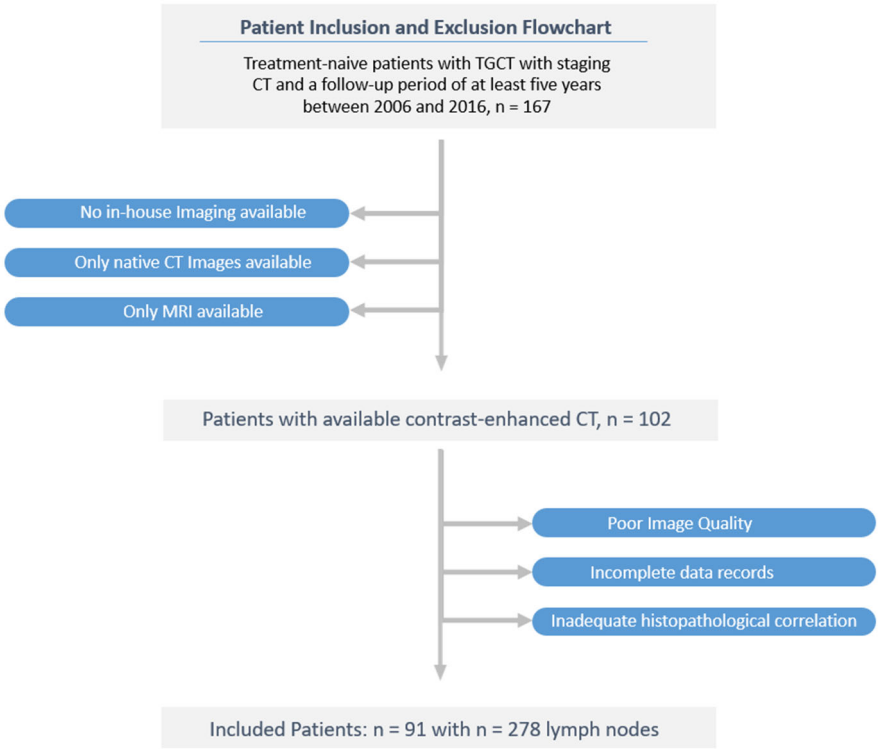

Figure 1. Recruitment pathway of the study.

Contrast-enhanced CT images for assessment of disease status were performed close to orchiectomy (+/- 2 weeks). The images were obtained as part of the routine staging on the multiple-row detector CT scanners Philips Brilliance CT 16-channel scanner or Philips Brilliance CT 64-channel scanner (Philips Healthcare, Cleveland, OH, USA). All CT imaging used the acquisition and reconstruction parameters according to the standard protocol: CT scans were performed after intravenous contrast agent injection of Ultravist® 370 (Bayer Schering Pharma, Berlin, Germany) in a weight-adopted dose with a delay of 70–80 s to represent the portovenous phase of chest and abdomen. Images were displayed in the axial plane with a section thickness of 2.0 - 5.0 mm with an in-plane resolution between 0.62×0.62 mm and 0.86×0.86 mm (tube voltage 100 kV–120 kV with automatically calculated tube current; matrix 512 × 512). By including different CT scanners, we aimed at a heterogeneous dataset for the most reasonable representation of a routine clinical scenario.

2.2. Segmentation and Radiomic Feature Extraction

Image-based texture analysis was first introduced in 1973 by Haralick et al. (36). Extracting texture parameters, such as the histogram features or features from the co-occurrence matrix or run-length matrix, have demonstrated their potential in recurrence risk stratification of many other cancer diseases (27,37).

Region-of-interest-segmentation, texture analysis and feature extraction were performed using the software mint Lesion™ (Version 3.8.4, mint Medical GmbH, Heidelberg, Germany), allowing three-dimensional size and, thus, whole lesion radiomic evaluation. Details regarding the extraction settings are listed in Appendix A, Table A1.

Two board-certified radiologists analysed all images, with over 10 years of experience in oncologic imaging and over 8-year experience in texture analysis.

Three retroperitoneal lymph nodes along the infrarenal aorta were segmented per patient resulting in 273 eligible samples randomly divided into a training set (n = 191) and a testing set (n = 82) at a ratio of 70:30.

Preprints (www.preprints.org) | NOT PEER-REVIEWED | Posted: 2 February 2023 doi:10.20944/preprints202302.0025.v1

In the final processing step, radiomic features were quantified concerning their characteristic pattern of grey levels within the ROI using texture feature descriptors according to the Image Biomarker Standardization Initiative (IBSI) guidelines (29).

A total of 85 imaging features were extracted from each ROI, including features related to the three-dimensional size and shape of the tumour, first-order statistics representing the distribution of voxel intensities within the selected region and texture-based features describing patterns of voxel intensities calculated from the grey-level co-occurrence matrix (GLCM) (see Tables A2 and A3 in Appendix A).

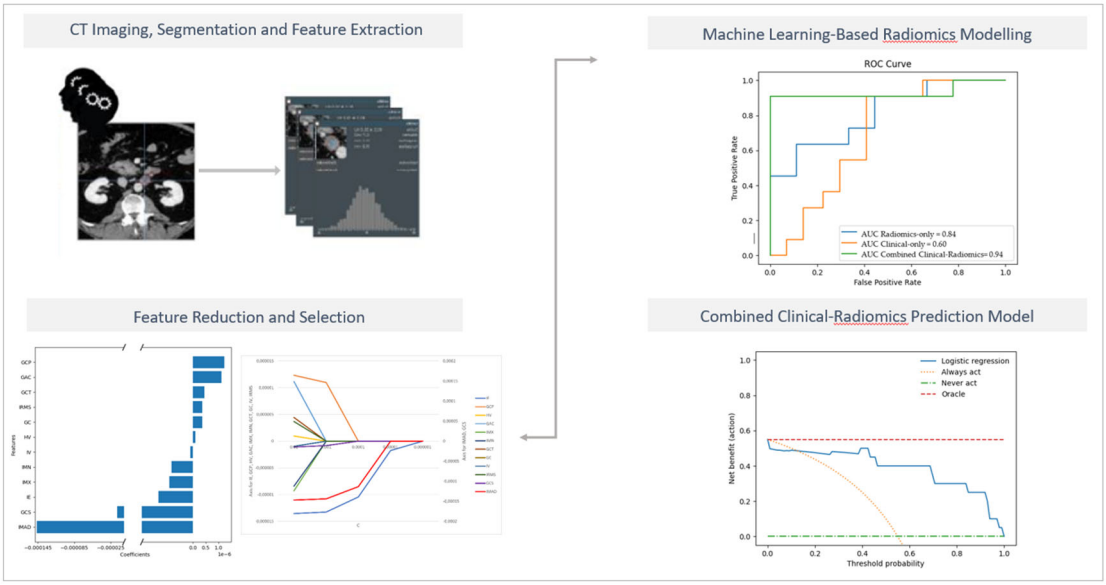

Figure 2. The schematic diagram for ROI segmentation and feature extraction used as input volume for model development. Details regarding the extraction settings are listed in Appendix A, Table A1.

2.3. Feature Selection and Development of the Predictive Radiomics Model

Like other data-mining applications, radiomics underlies the curse of dimensionality by extracting a great number of texture features from the regions of interest (ROIs) (38).

By choosing a subset of optimal features, overfitting is reduced, and thus models experience increased generalizability for faster and simpler machine learning models with improved performance (39).

In order to eliminate redundant radiomic features, feature selection was used by the least absolute shrinkage and selection operator (Lasso) logistic regression model (40,41).

Each feature has a related regression/covariate coefficient, and with a continuous increase in the λ value, some regression coefficients of the features continually decrease and trend toward 0. Lasso selected the remaining variables with non-zero as the most powerful prognostic features/valuable predictors to improve the prediction accuracy via penalized estimation functions.

To optimise the area under the receiver operating characteristic curve (AUC-ROC), we used tuning parameter (λ) selection and performed 10-fold cross-validation via minimum criteria. The model's optimum hyperparameters were found using grid search (42,43).

Multivariable logistic regression developed the most appropriate radiomics model by using the selected radiomic features as the input variables to classify between the binary output variables: Patients with LN metastases within the 6-year observation period were assigned to the high-risk group, whereas those with complete remission were classified in the low-risk group.

The under-sampled dataset was randomly divided into two partitions, training (70%) and testing (30%), respectively. To handle the imbalance between LN metastases (negative vs positive, 81/10) and avoid bias toward majority class cases to achieve a high classification rate, we applied the under-sampling technique "Instance Hardness Threshold (IHT)" to the training cohort (44,45). IHT is

Preprints (www.preprints.org) | NOT PEER-REVIEWED | Posted: 2 February 2023 doi:10.20944/preprints202302.0025.v1

a resampling approach that balances the dataset by reducing the number of data in the majority class by removing the majority class samples that overlap with the minority sample space.

The correlation coefficients and constant of the model were calculated (Figure 3, Appendix A Figure A1). It is worth noting that the feature selection by LASSO regression and the construction of the radiomics model were all from the date of the training cohort.

The Harrell concordance index (C-index) was measured to quantify the discrimination performance. Receiver operating characteristic (ROC) curves were plotted for each cohort; the AUC, accuracy, precision, recall, and F1-score were calculated to evaluate the classification ability in both the training and test sets.

The machine learning-based feature selection and the construction of the radiomics signature model were performed using our in-house software programmed with the Python Scikit-learn package (Python version 3.10, Scikit-learn version Scikit-learn 0.23.3, http://scikit-learn.org/) (42,46).

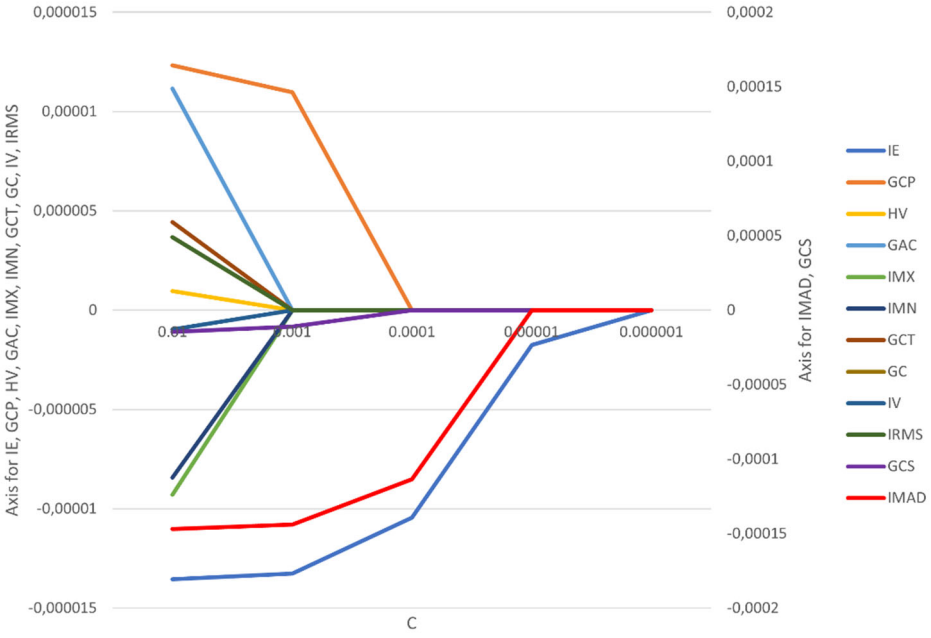

Figure 3. Feature weights generated by the LASSO logistic regression model's coefficients indicate positive or negative correlation with lymph node metastasis.

The features IMAD (Intensity Median Absolute Deviation) and GCS (GLCM Cluster Shade) use the secondary axis; all other features use the primary axis. The following are the abbreviations used for features:

IE – Intensity Energy
IMAD - Intensity Median Absolute Deviation
GCP - Glcm Cluster Prominence
GCS - Glcm Cluster Shade
HV - Histogram Variance
GAC - Glcm Auto Correlation
IMX - Intensity Maximum
IMN - Intensity Mean
GCT - Glcm Cluster Tendency
GC - Glcm Contrast
IV - Intensity Variance
IRMS - Root Mean Square

 doi:10.20944/preprints202302.0025.v1

2.4. Development of the Clinical and the Combined Prediction Models

The clinical factors included in our analysis were age, AFP level, B HCG level, histotype (seminoma and non-seminoma) and body mass index (BMI). These factors were included as they have all been suggested to be prognostic in TGCT (47–50). Our study included purely clinical and laboratory chemistry parameters to represent a real-life scenario for the individualized preoperative prediction of LNM at the time of the CT scan.

The selected clinical features and their relationship to lymph node metastasis were assessed with a univariable logistic regression algorithm in the training set. Variables with $p < 0.2$ from univariable analysis were included for further application in a multivariable logistic regression algorithm using forward stepwise selection. A cutoff value of 0.25 is supported by the literature (51,52).

Then, multivariable logistic regression analysis built three prediction models – a radiomics-only model, a clinical-only model and a combined clinical-radiomics model, incorporating the selected radiomics and clinical features.

Their predictive performance for detecting LN metastasis was assessed using the receiver operating characteristic curve (ROC) analysis, in which the areas under the curve (AUC), accuracy, precision and F1-Score were established.

The clinical utility was demonstrated by decision curve analysis (DCA) to evaluate the net benefits of the prediction models at different threshold probabilities in the training cohort and compare their discriminatory performance.

3. Results

3.1. Clinical Features

The study flowchart is presented in Figure 1.

Ninety-one consecutive patients with histologically-proven TGCT (mean age 35.2 ± 9.4 years, range 18–63) met the criteria for participation in the study. In this cohort, 10 patients (9.1%) relapsed within the six-year observation period (mean 9.8, 35.2 ± 9.4 years, range 18–63); There were no statistically significant differences in clinical characteristics between the LNM-positive group and LNM-negative group. After univariable LR analysis, age, AFP level, B HCG level, histotype and body mass index (BMI) were independent predictors in the clinical model. All patients' baseline clinical characteristics are summarised in Table 1.

Table 1. Baseline demographic and clinical data.

Average age (range)	35.2 ± 9.4 Years (18–63)
Histological type	
Seminoma	60 Patients (66 %)
Non-Seminoma	31 Patients (34%)
Tumour classification (T)	
T1a	64 (70%)
T1b	27 (30%)
Tumour Marker	
AFP positive	21 Patients (19%)
B HCG positive	40 Patients (44%)
AFP und B HCG positive	10 Patients (11%)
BMI (range)	25.9 ± 4.6 (19.3 –43.9)
Patients' status in 6-year follow up	
Complete remission (CR)	81 (89 %)
Relapse of disease (RD) with metastatic lymph nodes	10 (11 %)

Preprints (www.preprints.org) | NOT PEER-REVIEWED | Posted: 2 February 2023 doi:10.20944/preprints202302.0025.v1

In total, the dataset consisted of 273 sample instances (Three LN ROIs/patient) with 33 instances in the category "relapse of disease" (minority class) and 240 instances in the category "without relapse of disease" (majority class). According to a proportion of 7:3, the 273 sample instances were randomly divided into a training cohort (n = 191) and a test cohort (n = 82).

Due to the class imbalance in the dataset, the under-sampling technique called "Instance Hardness Threshold" was used to balance the data. The balanced data were used for the logistic regression machine learning mode.

3.1. Feature Selection and Performance of the Radiomics Prediction Model

A total of 85 radiomics features were extracted from the venous-phase CT images of the training cohort (Appendix A, Table A2). After screening these features, we chose the 12 radiomics features that had non-zero coefficients using the LASSO logistic regression model as the best-performing predictors for LN metastasis (Figure 3; Appendix A, Table A3).

These features were used as input volume for the machine learning-based radiomics modelling. Traditional measurements of machine learning-based modelling were used, including accuracy, precision, F1-Score, and the area under the ROC curve (AUC), to assess the performance of predicting lymph node metastases. All tests were two-sided; $p < 0.05$ was considered statistically significant.

In the ROC analysis of the radiomics model, the classification evaluation metrics of the 10-fold cross-validation were AUC 0.84 ± 0.17, accuracy 0.76 ± 0.12, precision 0.80 ± 0.18, recall 0.72 ± 0.23, and F1 score 0.73 ± 0.17 in the training cohort (Table 2).

3.2. Performance of the Clinical and the Combined Prediction Model

The clinical-only and combined clinical-radiomics models were built by applying multivariable logistic regression analysis.

The predictive performances of the radiomics-only, the clinical-only and the combined clinical-radiomics models on the training cohort are shown in Table 2.

The different models' overall accuracy and F1 score for predicting LN metastases were 77 % (range: 65–90%, AUC = 0.60–0.94) and 61% (range: 20–90%).

The combined clinical-radiomics model showed the best prediction accuracy with 90% (AUC 0.94–0.10), indicating that adding radiomics features could improve the predictive performance.

Figure 4 shows the receiver operating characteristic (ROC) curves for the clinical, the radiomics and the combined clinical-radiomics models on the training cohort.

Table 2. Performance of the radiomics, clinical, and combined models.

Model	AUC (95% CI)	Accuracy	Precision	Recall	F1 Score
Radiomics-only	0.84 ± 0.17	0.76 ± 0.12	0.80 ± 0.18	0.72 ± 0.23	0.73 ± 0.17
Clinical-only	0.60 ± 0.22	0.65 ± 0.11	0.14 ± 0.11	0.45 ± 0.46	0.20 ± 0.17
Combined Clinical-Radiomics	0.94 ± 0.10	0.90 ± 0.11	0.88 ± 0.15	0.94 ± 0.12	0.90 ± 0.11

Preprints (www.preprints.org) | NOT PEER-REVIEWED | Posted: 2 February 2023 doi:10.20944/preprints202302.0025.v1

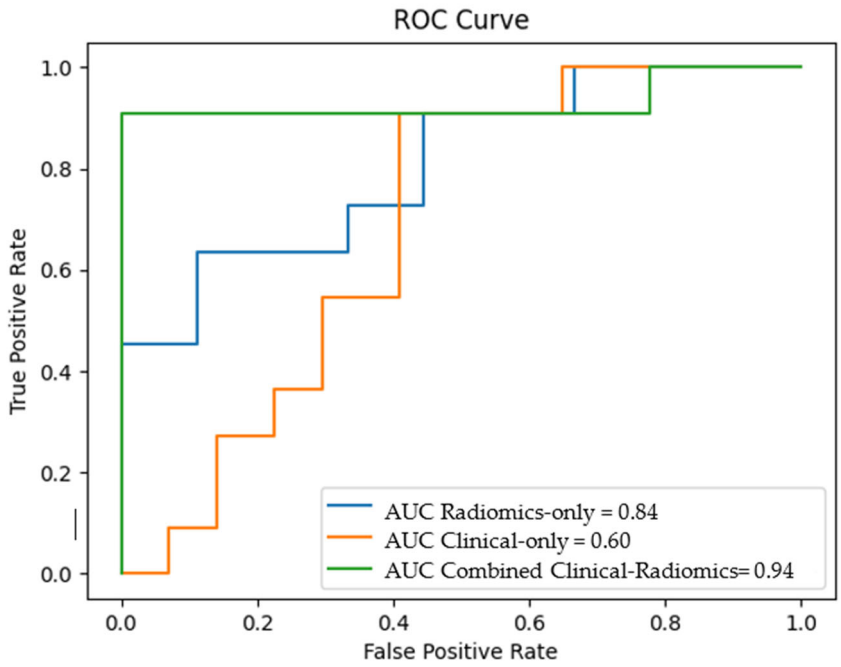

Figure 4. The ROC curves of the radiomics-only, the clinical-only and the combined clinical-radiomics models show that the combined model outperforms the radiomics and the clinical model in predicting LN metastasis (training cohort 94% vs 84% and 60%, respectively).

We performed a decision curve analysis to assess the clinical value of the combined clinical-radiomics model. Figure 5 illustrates the trade-offs between true positives and false positives regarding net benefit against threshold probability.

A decision curve analysis graph with threshold probability on the x-axis and net benefit on the y-axis illustrates the trade-offs between true positives and false positives, representing benefit and harm, respectively, as the threshold probability varies [83].

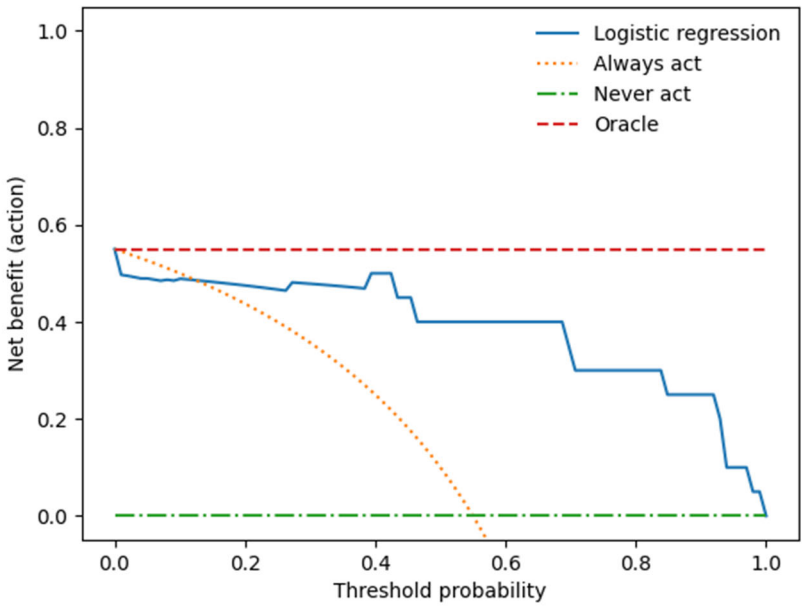

Figure 5. The decision curve analysis for the combined prediction model.

 doi:10.20944/preprints202302.0025.v1

The x-axis represents the threshold probability, the y-axis the net benefit; the blue line shows the combined prediction model. The green line represents the hypothesis that no patients had LN metastases, and the orange line that all patients had LN metastases. The threshold probability is where the treatment's expected benefit equals the benefit of avoiding treatment. If the possibility of LN metastasis is over the threshold probability, then a therapeutical strategy for LN metastases should be adopted. The DCA of the combined model shows that if the threshold possibility is between 0 and 0.13, then using the combined model to predict LNM adds more benefit than treating either or all patients.

4. Discussion

We developed a clinical-radiomics model for the individualized preoperative prediction of LNM in testicular germ cell tumour (TGCT) patients that consists of clinical risk factors and radiomics features to identify the stage I (TGCT) patients who require adjuvant therapy and those who do not.

Our main findings can be summarised by the following:

Using multivariable logistic regression analysis, we constructed a radiomics-only, a clinical-only, and a combined predictive model integrating clinical and radiomics features. The combined radiomics-clinical model showed the highest accuracy in predicting LNM (AUC = 0.94 ± 0.10; 95% CI); accuracy: 90%, precision 88%, recall 94%, and F1 score 90%.

Most newly diagnosed TGCT patients have stage I disease, characterized by the absence of malignancy outside the testis (53). Because >95% of men with stage I seminomas and non-seminomas are cured regardless of the treatment strategy used (54,55), the use of adjuvant chemotherapy for seminomas or non-seminomatous TGCTs, radiotherapy for seminomas and retroperitoneal lymph node dissection for non-seminomatous TGCTs after orchiectomy is debated due to short- and long-term side-effects including peripheral neuropathy, renal impairment, secondary malignancies and cardiovascular disease (5–7,56–60), and loss of antegrade ejaculation, small bowel obstruction and other complications (61,62)

For the clinical management of TGCTs, the serum biomarkers alpha-fetoprotein, human chorionic gonadotropin and lactate dehydrogenase are essential tools for diagnosis, prognosis, and surveillance of testicular cancer risk assessment (21,63) and have been integrated into the International Germ Cell Cancer Consensus Group consensus prognostic index for non-seminomatous classification (64). However, the sensitivity of these markers is limited, and the levels of these markers are usually "normal" in about 40% of men with disease recurrence (23).

Several studies have proposed further prognostic clinical risk factors, including age and BMI, but their role has not yet been sufficiently clarified, with somewhat controversial discussion (47–50).

Until now, neither imaging nor serum tumour markers nor clinical nomograms have been proven to be adequate predictors for the presence of lymph node metastases (24,25). On the other hand, suboptimal management gambles with the excellent outcomes of TGCT patients, either over- or undertreatment being equally harmful.

There are several studies applying radiomics to CT or MR images in order to classify LNs into benign and malignant LNs in lung cancer, oesophageal squamous cell carcinoma, tongue cancer, early breast cancer, lung cancer, gastric cancer, cervical cancer, endometrial cancer, bladder cancer and colorectal cancer – most of them MRI-based (33–35,65–69).

Although representing different tumour entities, classification accuracy in these studies falls between 76% and 84%, thus being lower in comparison to the results of our study, highlighting the potential of a radiomics-based approach for LN classification in different tumour entities.

Few studies exist on discriminating benign and malignant LNs in testicular cancer.

Baessler et al. demonstrated in their study that a (CT) radiomics–based machine learning classifier could predict the histopathology of lymph nodes after post-chemotherapy LN dissection in patients with metastatic non-seminomatous testicular germ cell tumours (70). This retrospective single-centre study, including 80 patients with a total of 204 lesions, used a support vector machine learning classifier, resulting in an accuracy of 81% for the discrimination of benign versus malignant histopathology.

 doi:10.20944/preprints202302.0025.v1

Nevertheless, in contrast to our study, they did not include clinical variables in their radiomics approach to further increase diagnostic performance.

Furthermore, they split the study cohort/dataset, which was altogether of moderate size, into three subgroups, with 63 patients in the training and only 19 patients in the test group. Researchers commonly split their data into test and validation sets to validate their findings. However, both test and validation sets subsequently have reduced sample sizes resulting in reduced statistical power compared to the initial cohort.

To overcome this, we used a cross-validation approach which employs repeated data splitting to prevent overfitting while simultaneously generating accurate estimates of the model coefficients (71).

The second study using a CT radiomics–based classifier to predict the dignity of LN metastases in patients with metastatic testicular germ cell tumours was published by Lewin et al. (72). This retrospective single-centre study, including 77 patients with a total of 102 lesions, used a support vector machine learning classifier, resulting in an accuracy of 72% for the discrimination of benign versus malignant histopathology, which was even lower than the classification results of Baessler et al.

Lewin et al. used only one single CT scanner. In contrast, our study analyzed data from two scanners, thus being more representative of data acquired during routine clinical practice. Like Baessler et al., Lewin et al. did not integrate clinical factors into a combined clinical-radiomics model.

Due to our 10-fold cross-validation approach, the a priori inhomogeneity of our dataset, and the integration of clinical risk factors, we are confident that our combined prediction model will generalize better to novel data. Thus, future prospective studies should further validate our trained model.

Several clinical models have been developed so far in order to predict the dignity of LN metastases. However, these models showed inconsistent results and have not been adopted yet for clinical decision-making (24,73–75).

Taken together, the identification and implementation of novel biomarkers might be helpful for early diagnosis and monitoring disease relapse.

This is the first study using a combined computed tomography (CT) radiomics models integrating clinical predictors for the individualized preoperative prediction of LNM in early-stage TGCT to reduce overtreatment in this group of young patients.

However, we acknowledge some limitations in the present study.

First, as a retrospective study with a modest cohort size, there may be inevitable selection bias. CT images were acquired with two different scanners. However, as discussed above, this heterogeneity represents routine clinical data reflecting a real-life setting, thus allowing for better generalizability of the trained model. Unlike prior radiomics investigations on LN metastasis that mostly extracted features from the largest cross-sectional area, our current study focused on the whole tumour analysis, which takes all the available slices into account, thus providing abundant information about tumour heterogeneity (34,59,76).

Second, the result of this study was from a single institution. Because of the high cure rate of stage I TGCTs, it is challenging to sufficiently power studies to examine prognostic and predictive factors. Hence, prospective and multicenter validation is warranted to obtain higher-level evidence in subsequent studies.

Third, only one (imaging) modality and the circulating tumour markers (β-subunit of human chorionic gonadotropin (β-HCG) and alpha-fetoprotein (AFP) were used in this study. In stage I seminoma, among other prognostic factors such as rete testis or lymphovascular invasion, tumour size is the most valuable prognostic factor for relapse

(77,78). Our study included solely clinical and laboratory parameters that can be collected easily, quickly, and non-invasively so that a preoperative risk assessment of the individual patient can already be made at the time of CT.

Beyond the protein-based tumour markers, a huge group of RNA molecules, so-called non-coding RNAs, show great potential as biomarkers (79). There is growing evidence that serum levels

 doi:10.20944/preprints202302.0025.v1

of stem cell-associated microRNAs (miR-371a-3p and miR-302/367 clusters) exceed conventional tumour markers in terms of sensitivity in detecting newly diagnosed TGCT patients (80,81).

If more modalities were combined as a multi-omics approach, the obtained feature pool might increase the ability to predict LNM in patients with testicular cancer.

Our presented CT-based radiomics-clinical model represents an exciting non-invasive prediction tool for individualized prediction of LN metastasis in testicular germ cell tumours to reduce overtreatment in this young group of patients. Multi-centre, retrospective validations and in fact prospective randomised clinical trials should be undertaken to gain high quality evidence for clinical applications in subsequent studies.

5. Conclusion

In conclusion, our combined clinical-radiomics model applied on preoperatively CT imaging represents an exciting new tool for improved prediction of lymph node metastases in early-stage testicular germ cell tumour (TGCT) patients to reduce overtreatment in this group of young patients. The presented approach should be combined with novel clinical biomarkers such as microRNAs (miR-371a-3p and miR-302/367 cluster) and further validated in larger, prospective clinical trials.

Author Contributions: Conceptualisation, C.S.L., F.Z., and C.G.L.; methodology, C.S.L., C.G.L. and M.G.; software, S.M., D.W. and M.G.; formal analysis, C.S.L. and C.G.L.; investigation, C.S.L., J.S. and C.G.L.; resources, C.S.L.; data curation, C.S.L., S.A.S., and C.G.L., writing—original draft preparation, C.S.L.; writing—review and editing, F.Z., S.A.S., M.B., D.W., and M.G.; visualisation, C.S.L., S.M., D.W., and C.G.L.; supervision, M.B.; project administration, C.S.L. All authors have read and agreed to the published version of the manuscript.

Funding: This research received no external funding.

Institutional Review Board Statement: The study was conducted in accordance with the Declaration of Helsinki and approved by the ethics committee of the medical faculty of the University of Ulm (protocol code 155/18, 25 April 2018).

Informed Consent Statement: Informed consent was obtained from all subjects involved in the study.

Data Availability Statement: Data sharing is not applicable to this article.

Conflicts of Interest: The authors declare no conflict of interest.

Abbreviations

AFP	Alpha-fetoprotein
AUC	Area under the curve
CT	Computed tomography
hCG	Human chorionic gonadotropin
LNs	Lymph nodes
LNM	Lymph node metastases
LR	Logistic regression
ML	Machine learning
ROC	Receiver operating curve
ROI	Region of interest
TGCT	Testicular germ cell tumour

Preprints (www.preprints.org) | NOT PEER-REVIEWED | Posted: 2 February 2023 doi:10.20944/preprints202302.0025.v1

Appendix A

Table A1. Settings of the radiomics feature extraction.

Setting	Determination
Bin Method	FBN
Bin Amount	32
LoG Filter	0
LoG Sigma	2
Matrix Aggregation Method	3D Average Directions
Resample Filter	1
Resample Spacing X	1
Resample Spacing Y	1
Resample Spacing Z	1
Second-Order Distance	1
Threshold Filter	0

Table A2. Radiomics features extracted for model development.

Radiomics Features of First Order	Radiomics Features of Second Order: Gray Level Co-Occurrence Matrix (GLCM)
Histogram Minimum	Joint Maximum
Histogram Maximum	Joint Average
Histogram Range	Standart Deviation
Histogram Mean	Joint Variance
Histogram Variance	Joint Entropy
Histogram Standart Deviation	Difference Average
Histogram Skewness	Difference Variance
Histogram Kurtosis	Difference Entropy
Histogram Entropy	Sum of Averages
Histogram Uniformity	Sum of Variance
Histogram Mean Absolute Deviation	Sum of Entropy
Histogram Robust Mean Absolute Deviation	Angular Second Moment
Histogram Median Absolute Deviation	Contrast
Histogram Coefficient Variation	Dissimilarity
Histogram Quartile Coefficient Dispersion	Inverse Difference
Histogram Interquartile Range	Inverse Difference Normalised
Histogram P10th	Inverse Difference Moment
Histogram P25th	Inverse Difference Moment Normalised
Histogram P50th	Joint Maximum
Histogram P75th	Joint Average
Histogram P90th	Standart Deviation
Histogram Minimum Histogram Gradient Intensity	Joint Variance
Histogram MaximumHistogram Gradient Intensity	Joint Entropy
Intensity Minimum	Difference Average
Intensity Maximum	Difference Variance
Intensity Range	Difference Entropy
Intensity Mean	Sum of Averages
Intensity Variance	Sum of Variance
Intensity Standart Deviation	Sum of Entropy
Intensity Skewness	Angular Second Moment
Intensity Kurtosis	Contrast
Intensity Energy	Dissimilarity

Preprints (www.preprints.org) | NOT PEER-REVIEWED | Posted: 2 February 2023 doi:10.20944/preprints202302.0025.v1

Intensity P10th	Inverse Variance
Intensity P25th	Correlation
Intensity P50th	Auto Correlation
Intensity P75th	Cluster Shade
Intensity P90th	Cluster Prominence
Intensity Root Mean Square	Cluster Tendency
Intensity Mean Absolute Deviation	Information Correlation 1
Intensity Robust Mean Absolute Deviation	Information Correlation 2
Intensity Median Absolute Deviation	Inverse Variance 41
Intensity Coefficient Variation	
Intensity Quartile Coefficient Dispersion	
Intensity Interquartile Range 44	

Table A3. Radiomics features selected by LASSO.

Radiomics Features of First Order	**Radiomics Features of Second Order: Gray Level Co-Occurrence Matrix (GLCM)**
Histogram Variance	Auto Correlation
Intensity Maximum	Cluster Shade
Intensity Mean	Cluster Prominence
Intensity Variance	Cluster Tendency
Intensity Energy	Contrast
Intensity Root Mean Square	
Intensity Median Absolute Deviation	

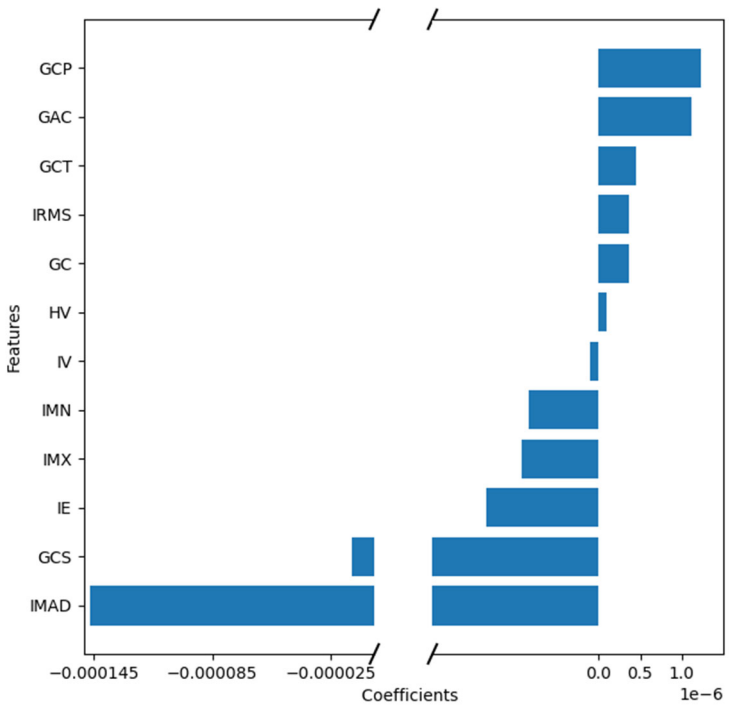

Figure A1. Feature weights generated by the coefficients of the logistic regression model indicating positive or negative correlation with lymph node metastasis.

References

1. Ruf CG, Isbarn H, Wagner W, Fisch M, Matthies C, Dieckmann KP. Changes in epidemiologic features of testicular germ cell cancer: age at diagnosis and relative frequency of seminoma are constantly and significantly increasing. In Elsevier; 2014. p. 33-e1.
2. Bray F, Richiardi L, Ekbom A, Pukkala E, Cuninkova M, Møller H. Trends in testicular cancer incidence and mortality in 22 European countries: continuing increases in incidence and declines in mortality. International journal of cancer. 2006;118(12):3099–111.
3. Einhorn LH. Treatment of testicular cancer: a new and improved model. Journal of clinical oncology. 1990;8(11):1777–81.
4. Kollmannsberger C, Tandstad T, Bedard PL, Cohn-Cedermark G, Chung PW, Jewett MA, et al. Patterns of relapse in patients with clinical stage I testicular cancer managed with active surveillance. J Clin Oncol. 2015;33(1):51–7.
5. Fung C, Sesso HD, Williams AM, Kerns SL, Monahan P, Zaid MA, et al. Multi-institutional assessment of adverse health outcomes among North American testicular cancer survivors after modern cisplatin-based chemotherapy. Journal of Clinical Oncology. 2017;35(11):1211.
6. Huddart R, Norman A, Shahidi M, Horwich A, Coward D, Nicholls J, et al. Cardiovascular disease as a long-term complication of treatment for testicular cancer. Journal of Clinical Oncology. 2003;21(8):1513–23.
7. Travis LB, Ng AK, Allan JM, Pui CH, Kennedy AR, Xu XG, et al. Second malignant neoplasms and cardiovascular disease following radiotherapy. Journal of the National Cancer Institute. 2012;104(5):357–70.
8. Kerns SL, Fung C, Monahan PO, Ardeshir-Rouhani-Fard S, Zaid MIA, Williams AM, et al. Cumulative burden of morbidity among testicular cancer survivors after standard cisplatin-based chemotherapy: a multi-institutional study. Journal of Clinical Oncology. 2018;36(15):1505.
9. Agrawal V, Dinh Jr PC, Fung C, Monahan PO, Althouse SK, Norton K, et al. Adverse health outcomes among US testicular cancer survivors after cisplatin-based chemotherapy vs surgical management. JNCI cancer spectrum. 2020;4(2):pkz079.
10. Tandstad T, Kollmannsberger CK, Roth BJ, Jeldres C, Gillessen S, Fizazi K, et al. Practice makes perfect: the rest of the story in testicular cancer as a model curable neoplasm. Journal of Clinical Oncology. 2017;35(31):3525.
11. Rajpert-De Meyts E, McGlynn KA, Okamoto K, Jewett MA, Bokemeyer C. Testicular germ cell tumours. The Lancet. 2016;387(10029):1762–74.
12. Cheng L, Albers P, Berney DM, Feldman DR, Daugaard G, Gilligan T, et al. Testicular cancer. Nature Reviews Disease Primers. 2018;4(1):1–24.
13. Dieckmann KP, Simonsen-Richter H, Kulejewski M, Anheuser P, Zecha H, Isbarn H, et al. Serum tumour markers in testicular germ cell tumours: frequencies of elevated levels and extents of marker elevation are significantly associated with clinical parameters and with response to treatment. BioMed Research International. 2019;2019.
14. Gilligan TD, Hayes DF, Seidenfeld J, Temin S. ASCO clinical practice guideline on uses of serum tumor markers in adult males with germ cell tumors. Journal of oncology practice. 2010;6(4):199.
15. Patel HD, Joice GA, Schwen ZR, Semerjian A, Alam R, Srivastava A, et al. Retroperitoneal lymph node dissection for testicular seminomas: population-based practice and survival outcomes. World J Urol. 2018 Jan 1;36(1):73–8.
16. Albers P, Siener R, Kliesch S, Weissbach L, Krege S, Sparwasser C, et al. Risk factors for relapse in clinical stage I nonseminomatous testicular germ cell tumors: results of the German Testicular Cancer Study Group Trial. Journal of clinical oncology. 2003;21(8):1505–12.
17. Chung P, Daugaard G, Tyldesley S, Atenafu EG, Panzarella T, Kollmannsberger C, et al. Evaluation of a prognostic model for risk of relapse in stage I seminoma surveillance. Cancer medicine. 2015;4(1):155–60.
18. Nichols CR, Roth B, Albers P, Einhorn LH, Foster R, Daneshmand S, et al. Active surveillance is the preferred approach to clinical stage I testicular cancer. Journal of Clinical Oncology. 2013;31(28):3490–3.
19. Hale GR, Teplitsky S, Truong H, Gold SA, Bloom JB, Agarwal PK. Lymph node imaging in testicular cancer. Translational Andrology and Urology. 2018;7(5):864.
20. Hudolin T, Kastelan Z, Knezevic N, Goluza E, Tomas D, Coric M. Correlation between retroperitoneal lymph node size and presence of metastases in nonseminomatous germ cell tumors. International Journal of Surgical Pathology. 2012;20(1):15–8.

21. Murray MJ, Huddart RA, Coleman N. The present and future of serum diagnostic tests for testicular germ cell tumours. Nature Reviews Urology. 2016;13(12):715–25.
22. Albers P, Albrecht W, Algaba F, Bokemeyer C, Cohn-Cedermark G, Fizazi K, et al. EAU Guidelines on Testicular Cancer: 2011 Update. European Urology. 2011 Aug 1;60(2):304–19.
23. Trigo JM, Tabernero JM, Paz-Ares L, García-Llano JL, Mora J, Lianes P, et al. Tumor markers at the time of recurrence in patients with germ cell tumors. Cancer. 2000;88(1):162–8.
24. Steyerberg E, Gerl A, Fossa S, Sleijfer D, de Wit R, Kirkels W, et al. Validity of predictions of residual retroperitoneal mass histology in nonseminomatous testicular cancer. Journal of clinical oncology. 1998;16(1):269–74.
25. Vergouwe Y, STEYERBERG EW, FOSTER RS, HABBEMA JDF, DONOHUE JP. Validation of a prediction model and its predictors for the histology of residual masses in nonseminomatous testicular cancer. The Journal of urology. 2001;165(1):84–8.
26. Obermeyer Z, Emanuel EJ. Predicting the future—big data, machine learning, and clinical medicine. The New England journal of medicine. 2016;375(13):1216.
27. Lambin P, Leijenaar RT, Deist TM, Peerlings J, De Jong EE, Van Timmeren J, et al. Radiomics: the bridge between medical imaging and personalized medicine. Nature reviews Clinical oncology. 2017;14(12):749–62.
28. Gillies RJ, Kinahan PE, Hricak H. Radiomics: images are more than pictures, they are data. Radiology. 2016;278(2):563.
29. Zwanenburg A, Vallières M, Abdalah MA, Aerts HJ, Andrearczyk V, Apte A, et al. The image biomarker standardization initiative: standardized quantitative radiomics for high-throughput image-based phenotyping. Radiology. 2020;295(2):328–38.
30. Sollini M, Antunovic L, Chiti A, Kirienko M. Towards clinical application of image mining: a systematic review on artificial intelligence and radiomics. European journal of nuclear medicine and molecular imaging. 2019;46(13):2656–72.
31. Ibrahim A, Primakov S, Beuque M, Woodruff H, Halilaj I, Wu G, et al. Radiomics for precision medicine: Current challenges, future prospects, and the proposal of a new framework. Methods. 2021;188:20–9.
32. Dong D, Tang L, Li ZY, Fang MJ, Gao JB, Shan XH, et al. Development and validation of an individualized nomogram to identify occult peritoneal metastasis in patients with advanced gastric cancer. Annals of Oncology. 2019;30(3):431–8.
33. Huang Y qi, Liang C hong, He L, Tian J, Liang C shan, Chen X, et al. Development and validation of a radiomics nomogram for preoperative prediction of lymph node metastasis in colorectal cancer. Journal of clinical oncology. 2016;34(18):2157–64.
34. Wu S, Zheng J, Li Y, Yu H, Shi S, Xie W, et al. A Radiomics Nomogram for the Preoperative Prediction of Lymph Node Metastasis in Bladder CancerA Radiomics Nomogram for Bladder Cancer. Clinical Cancer Research. 2017;23(22):6904–11.
35. Gao J, Han F, Jin Y, Wang X, Zhang J. A radiomics nomogram for the preoperative prediction of lymph node metastasis in pancreatic ductal adenocarcinoma. Frontiers in oncology. 2020;10:1654.
36. Haralick RM, Shanmugam K, Dinstein IH. Textural features for image classification. IEEE Transactions on systems, man, and cybernetics. 1973;(6):610–21.
37. Shen C, Liu Z, Guan M, Song J, Lian Y, Wang S, et al. 2D and 3D CT radiomics features prognostic performance comparison in non-small cell lung cancer. Translational oncology. 2017;10(6):886–94.
38. Duin RP, Pekalska E. Dissimilarity Representation For Pattern Recognition, The: Foundations And Applications. Vol. 64. World scientific; 2005.
39. Sánchez-Maroño N, Alonso-Betanzos A, Tombilla-Sanromán M. Filter methods for feature selection–a comparative study. In Springer; 2007. p. 178–87.
40. Tibshirani R. The lasso method for variable selection in the Cox model. Statistics in medicine. 1997;16(4):385–95.
41. Tibshirani R. Regression shrinkage and selection via the lasso: a retrospective. Journal of the Royal Statistical Society: Series B (Statistical Methodology). 2011;73(3):273–82.
42. Pedregosa F, Varoquaux G, Gramfort A, Michel V, Thirion B, Grisel O, et al. Scikit-learn: Machine learning in Python. the Journal of machine Learning research. 2011;12:2825–30.

43. Agrawal T. Hyperparameter Optimization Using Scikit-Learn. In: Hyperparameter Optimization in Machine Learning: Make Your Machine Learning and Deep Learning Models More Efficient [Internet]. Berkeley, CA: Apress; 2021. p. 31–51. Available from: https://doi.org/10.1007/978-1-4842-6579-6_2
44. Smith MR, Martinez T, Giraud-Carrier C. An instance level analysis of data complexity. Machine learning. 2014;95(2):225–56.
45. Lemaitre G, Nogueira F, Oliveira D, Aridas C. imbalanced-learn 0.1.
46. van Rossum G, Drake FL. Python/C API Manual-Python 2.6. 2009;
47. Fosså SD, Cvancarova M, Chen L, Allan AL, Oldenburg J, Peterson DR, et al. Adverse prognostic factors for testicular cancer–specific survival: a population-based study of 27,948 patients. Journal of Clinical Oncology. 2011;29(8):963–70.
48. Parker C, Milosevic M, Panzarella T, Banerjee D, Jewett M, Catton C, et al. The prognostic significance of the tumour infiltrating lymphocyte count in stage I testicular seminoma managed by surveillance. European Journal of Cancer. 2002;38(15):2014–9.
49. Lerro C, McGlynn K, Cook M. A systematic review and meta-analysis of the relationship between body size and testicular cancer. British journal of cancer. 2010;103(9):1467–74.
50. Dieckmann KP, Hartmann JT, Classen J, Diederichs M, Pichlmeier U. Is increased body mass index associated with the incidence of testicular germ cell cancer? Journal of cancer research and clinical oncology. 2009;135(5):731–8.
51. Mickey RM, Greenland S. The impact of confounder selection criteria on effect estimation. American journal of epidemiology. 1989;129(1):125–37.
52. Bendel RB, Afifi AA. Comparison of stopping rules in forward "stepwise" regression. Journal of the American Statistical association. 1977;72(357):46–53.
53. Powles TB, Bhardwa J, Shamash J, Mandalia S, Oliver T. The changing presentation of germ cell tumours of the testis between 1983 and 2002. BJU international. 2005;95(9):1197–200.
54. Oldenburg J, Fosså S, Nuver J, Heidenreich A, Schmoll HJ, Bokemeyer C, et al. Testicular seminoma and non-seminoma: ESMO Clinical Practice Guidelines for diagnosis, treatment and follow-up. Annals of Oncology. 2013;24:vi125–32.
55. Albers P, Siener R, Kliesch S, Weissbach L, Krege S, Sparwasser C, et al. Risk factors for relapse in clinical stage I nonseminomatous testicular germ cell tumors: results of the German Testicular Cancer Study Group Trial. Journal of clinical oncology. 2003;21(8):1505–12.
56. Kier MG, Hansen MK, Lauritsen J, Mortensen MS, Bandak M, Agerbaek M, et al. Second malignant neoplasms and cause of death in patients with germ cell cancer: a Danish nationwide cohort study. JAMA oncology. 2016;2(12):1624–7.
57. Fung C, Fossa SD, Milano MT, Sahasrabudhe DM, Peterson DR, Travis LB. Cardiovascular Disease Mortality After Chemotherapy or Surgery for Testicular Nonseminoma: A Population-Based Study. J Clin Oncol. 2015 Oct 1;33(28):3105–15.
58. Fung C, Fossa SD, Williams A, Travis LB. Long-term morbidity of testicular cancer treatment. Urologic Clinics. 2015;42(3):393–408.
59. Kim C, McGlynn KA, McCorkle R, Erickson RL, Niebuhr DW, Ma S, et al. Quality of life among testicular cancer survivors: a case–control study in the United States. Quality of Life Research. 2011;20(10):1629–37.
60. Lauritsen J, Kier MG, Mortensen MS, Bandak M, Gupta R, Holm NV, et al. Germ cell cancer and multiple relapses: toxicity and survival. Journal of Clinical Oncology. 2015;33(28):3116–23.
61. Baniel J, Sella A. Complications of retroperitoneal lymph node dissection in testicular cancer: primary and post-chemotherapy. Semin Surg Oncol. 1999 Dec;17(4):263–7.
62. Heidenreich A, Thüer D, Polyakov S. Postchemotherapy Retroperitoneal Lymph Node Dissection in Advanced Germ Cell Tumours of the Testis. European Urology. 2008 Feb 1;53(2):260–74.
63. Lobo J, Leão R, Jerónimo C, Henrique R. Liquid biopsies in the clinical management of germ cell tumor patients: state-of-the-art and future directions. International Journal of Molecular Sciences. 2021;22(5):2654.
64. Eyben FE von. Laboratory markers and germ cell tumors. Critical reviews in clinical laboratory sciences. 2003;40(4):377–427.
65. Li K, Yao Q, Xiao J, Li M, Yang J, Hou W, et al. Contrast-enhanced CT radiomics for predicting lymph node metastasis in pancreatic ductal adenocarcinoma: a pilot study. Cancer Imaging. 2020;20(1):1–10.

66. Yan BC, Li Y, Ma FH, Zhang GF, Feng F, Sun MH, et al. Radiologists with MRI-based radiomics aids to predict the pelvic lymph node metastasis in endometrial cancer: a multicenter study. Eur Radiol. 2021 Jan 1;31(1):411–22.
67. Wu Q, Wang S, Chen X, Wang Y, Dong L, Liu Z, et al. Radiomics analysis of magnetic resonance imaging improves diagnostic performance of lymph node metastasis in patients with cervical cancer. Radiotherapy and Oncology. 2019 Sep 1;138:141–8.
68. Xiao M, Ma F, Li Y, Li Y, Li M, Zhang G, et al. Multiparametric MRI-Based Radiomics Nomogram for Predicting Lymph Node Metastasis in Early-Stage Cervical Cancer. Journal of Magnetic Resonance Imaging. 2020;52(3):885–96.
69. Andersen MB, Harders SW, Ganeshan B, Thygesen J, Torp Madsen HH, Rasmussen F. CT texture analysis can help differentiate between malignant and benign lymph nodes in the mediastinum in patients suspected for lung cancer. Acta Radiol. 2016 Jun 1;57(6):669–76.
70. Baessler B, Nestler T, Pinto dos Santos D, Paffenholz P, Zeuch V, Pfister D, et al. Radiomics allows for detection of benign and malignant histopathology in patients with metastatic testicular germ cell tumors prior to post-chemotherapy retroperitoneal lymph node dissection. European Radiology. 2020;30(4):2334–45.
71. Harrell Jr FE, Lee KL, Mark DB. Multivariable prognostic models: issues in developing models, evaluating assumptions and adequacy, and measuring and reducing errors. Statistics in medicine. 1996;15(4):361–87.
72. Lewin J, Dufort P, Halankar J, O'Malley M, Jewett MA, Hamilton RJ, et al. Applying radiomics to predict pathology of postchemotherapy retroperitoneal nodal masses in germ cell tumors. JCO Clinical Cancer Informatics. 2018;2:1–12.
73. Leão R, Nayan M, Punjani N, Jewett MAS, Fadaak K, Garisto J, et al. A New Model to Predict Benign Histology in Residual Retroperitoneal Masses After Chemotherapy in Nonseminoma. European Urology Focus. 2018 Dec 1;4(6):995–1001.
74. Vergouwe Y, Steyerberg EW, Foster RS, Sleijfer DT, Fosså SD, Gerl A, et al. Predicting Retroperitoneal Histology in Postchemotherapy Testicular Germ Cell Cancer: A Model Update and Multicentre Validation with More Than 1000 Patients. European Urology. 2007 Feb 1;51(2):424–32.
75. ALBERS PETER, WEISSBACH LOTHAR, KREGE SUSANNE, KLIESCH SABINE, HARTMANN MICHAEL, HEIDENREICH AXEL, et al. Prediction of Necrosis After Chemotherapy of Advanced Germ Cell Tumors: Results of a Prospective Multicenter Trial of the German Testicular Cancer Study Group. Journal of Urology. 2004 May 1;171(5):1835–8.
76. Ng F, Ganeshan B, Kozarski R, Miles KA, Goh V. Assessment of Primary Colorectal Cancer Heterogeneity by Using Whole-Tumor Texture Analysis: Contrast-enhanced CT Texture as a Biomarker of 5-year Survival. Radiology. 2013 Jan;266(1):177–84.
77. Zengerling F, Kunath F, Jensen K, Ruf C, Schmidt S, Spek A. Prognostic factors for tumor recurrence in patients with clinical stage I seminoma undergoing surveillance—A systematic review. Urologic Oncology: Seminars and Original Investigations. 2018 Oct 1;36(10):448–58.
78. Zengerling F, Beyersdorff D, Busch J, Heinzelbecker J, Pfister D, Ruf C, et al. Prognostic factors in patients with clinical stage I nonseminoma—beyond lymphovascular invasion: a systematic review. World J Urol. 2022 Dec 1;40(12):2879–87.
79. Smolle MA, Calin HN, Pichler M, Calin GA. Noncoding RNAs and immune checkpoints—clinical implications as cancer therapeutics. The FEBS Journal. 2017;284(13):1952–66.
80. Dieckmann KP, Radtke A, Spiekermann M, Balks T, Matthies C, Becker P, et al. Serum Levels of MicroRNA miR-371a-3p: A Sensitive and Specific New Biomarker for Germ Cell Tumours. European Urology. 2017 Feb 1;71(2):213–20.
81. Bezan A, Gerger A, Pichler M. MicroRNAs in testicular cancer: implications for pathogenesis, diagnosis, prognosis and therapy. Anticancer research. 2014;34(6):2709–13.